DOI: 10.1002/chem.201001306

Electron Attachment to a Hydrated DNA Duplex: The Dinucleoside Phosphate Deoxyguanylyl-3′,5′-Deoxycytidine

Jiande Gu,*[a] Ning-Bew Wong,[b] Yaoming Xie,[c] and F. Henry Schaefer, III*[c]

Abstract: The minimal essential section of DNA helices, the dinucleoside phosphate deoxyguanylyl-3′,5′-deoxycytidine dimer octahydrate, $[dGpdC]_2$, has been constructed, fully optimized, and analyzed by using quantum chemical methods at the B3LYP/6-31+G(d,p) level of theory. Study of the electrons attached to $[dGpdC]_2$ reveals that DNA double strands are capable of capturing low-energy electrons and forming electronically stable radical anions. The relatively large vertical electron affinity (VEA) predicted for $[dGpdC]_2$ (0.38 eV) indicates that the cytosine bases are good electron captors in DNA double strands. The structure, charge distribution, and molecular orbital analysis for the fully optimized radical anion $[dGpdC]_2^{\bullet-}$ suggest that the extra electron tends to be redistributed to one of the cytosine base moieties, in an electronically stable structure (with adiabatic electron affinity (AEA) 1.14 eV and vertical detachment energy (VDE) 2.20 eV). The structural features of the optimized radical anion $[dGpdC]_2^{\bullet-}$ also suggest the probability of interstrand proton transfer. The interstrand proton transfer leads to a distonic radical anion $[d(G-H)pdC:d(C+H)pdG]^{\bullet-}$, which contains one deprotonated guanine anion and one protonated cytosine radical. This distonic radical anion is predicted to be more stable than $[dGpdC]_2^{\bullet-}$. Therefore, experimental evidence for electron attachment to the DNA double helices should be related to $[d(G-H)pdC:d(C+H)pdG]^{\bullet-}$ complexes, for which the VDE might be as high as 2.7 eV (in dry conditions) to 3.3 eV (in fully hydrated conditions). Effects of the polarizable medium have been found to be important for increasing the electron capture ability of the dGpdC dimer. The ultimate AEA value for cytosine in DNA duplexes is predicted to be 2.03 eV in aqueous solution.

Keywords: computational chemistry · DNA · electron affinity · electron transfer · helical structures · proton transfer

Introduction

Electron attachment to DNA fragments has been found to be related to biochemical processes of vital importance, such as DNA damage and repair,[1–8] charge transfer along DNA,[9–13] and the initiation of reactions leading to mutation.[1,3,14] Knowledge of the distribution of excess electron sites for DNA strands is fundamental for understanding the mechanism of these DNA-related chemical reactions.[8,15–18] The study of electron attachment to DNA, RNA, and their subunits has received increasing attention since 1990.

Experiment-based investigations suggest that the pyrimidine nucleobases have small electron affinities (EAs): ≈0.1 eV for thymine (T), cytosine (C), and uracil (U).[19,20] Gas-phase experimental studies have revealed negative EA values for adenine (A) and C.[21–24] Recently, photoelectron spectroscopy has detected anionic states of tautomers of adenine and guanine (G). The radical anions of the tautomers exhibit relatively large vertical electron detachment energies (VDEs).[24,25] The photoelectron spectra of the anionic base pairs of adenine and thymine (AT^-) and 9-methyladenine and 1-methylthymine ($mAmT^-$) reveal a large VDE (0.7–1.7 eV) for the radical anions of these base pairs.[26] Compared to the reliable theoretical prediction of the VDE of

[a] Prof. J. Gu
Drug Design & Discovery Center
State Key Laboratory of Drug Research
Shanghai Institute of Materia Medica
Shanghai Institutes for Biological Sciences, CAS
Shanghai 201203 (P. R. China)
Fax: (+86) 21-50807088
E-mail: jiande@icnanotox.org

[b] Prof. N.-B. Wong
Department of Biology and Chemistry
City University of Hong Kong
Kowloon (Hong Kong)

[c] Dr. Y. Xie, Prof. F. H. Schaefer, III
Center for Computational Quantum Chemistry
University of Georgia
Athens, 30602-2525 (USA)
Fax: (+1) 706-542-0406
E-mail: sch@uga.edu

the canonical form of the radical anion $AT^{\bullet-}$ (0.64 eV),[27] the large VDE reported for AT^- (1.7 eV) strongly suggests that this base pair adopts a tautomeric form under the experimental conditions. Electron attachment energies of the radical anions of nucleosides have also been determined by Bowen's group.[28] These experimental electron affinity values for thymidine, cytidine, and adenosine are within 0.2 eV of the previously reported theoretical predictions.[16] However, experiments on the electron-capturing efficiencies of short DNA oligomers provide only estimates of the relative order of the vertical attachment energies (or VEAs) for DNA single strands.[15]

Theoretical investigations at various levels of sophistication have complemented experimental explorations. The coupled cluster level of theory with single, double, and perturbative triple excitations (CCSD(T)) successfully elucidated the tautomeric forms of the covalently bound radical anions of guanine[25,29] and adenine.[24] The most reliable density functional theory (DFT) approaches yield AEAs of individual nucleic acid bases that are consistent with the best experiments.[30–32] Step-by-step, with the extensively calibrated B3LYP/DZP++ approach,[33] a reliable data bank of the electron affinities of the 2′-deoxyribonucleosides (the predicted AEAs and VDEs have recently been confirmed by photoelectron spectroscopic experiments),[18,28] the nucleotides (3′-dCMP, 3′-dTMP, 5′-dCMP, 5′-dTMP),[8,17,35,36] and the nucleoside-3′,5′-diphosphates (3′,5′-dGDP, 3′,5′-dADP, 3′,5′-dCDP, and 3′,5′-dTDP)[18] has been established. Theoretical studies of electron attachment to DNA have been extended to the prediction of the electron affinities of hydrogen-bonding paired DNA subunits, such as nucleobase pairs (A:T and G:C pairs),[26,37–40] nucleoside pairs (dA:dT and dG:dC),[41,42] and at least one nucleotide–nucleobase pair.[43] The DFT approach has also been applied to elucidate the electron-capture abilities of the A:T and mA:mT pairs in their tautomeric forms.[26] The influence of water microsolvation on electron attachment to nucleobases has also been investigated extensively at different levels of theory.[44–57] Recently, the electron affinities of thymine–adenine and guanine–cytosine base pairs stacking between different bases were studied by the resolution of identity MP2 (RI-MP2) approach.[58,59]

As a crucial step in achieving a realistic description of electron attachment to nucleotide oligomers, dinucleoside phosphate deoxycytidylyl-3′,5′-deoxyguanosine (dCpdG), dinucleoside phosphate deoxyguanylyl-3′,5′-deoxycytidine (dGpdC), dinucleoside phosphate deoxythytidylyl-3′,5′-deoxyadenosine (dTpdA), dinucleoside phosphate deoxyadenylyl-3′,5′-deoxythytidine (dApdT), and the corresponding radical anions have been investigated theoretically in our laboratories.[60] The studies of these systems have allowed the most complete descriptions to date of the minimum length of chain in single-strand DNA, and have provided stepping-stones for understanding electron attachment to single-strand DNA.

Here we report the latest developments in theoretical studies of the DNA duplex: electron attachment to the double helix of dinucleoside phosphate deoxyguanylyl-3′,5′-deoxycytidine (dGpdC dimer, see Scheme 1). To achieve a realistic description of the DNA duplex, eight hydration

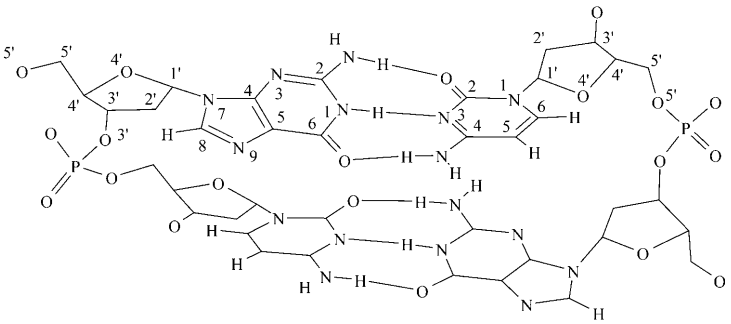

Scheme 1. Model of the DNA duplex: double helix of dinucleoside phosphate deoxyguanylyl-3′,5′-deoxycytidine ($[dGpdC]_2$). Hydrogen atoms attached to the ribose-phosphate backbones have been omitted for clarity.

water molecules have been included in the model system in such a way that the water molecules are able to form proper hydrogen-bonding patterns with the bases. The importance of the existence of hydration water molecules has been demonstrated in computational studies of the double-stranded model of deoxyadenylyl-3′,5′-deoxyuridine.[61] This minimal segment of the DNA double-helical complex dGpdC dimer octahydrate contains all the most crucial stabilization factors, such as base–base, base–backbone, and hydration interactions. Thus, exploring such complexes is expected to provide key information concerning electron attachment to the DNA double strand.

Computational Methods

One important conclusion from previous studies of electron attachment to the nucleotide oligomers dCpdG and dGpdC is that the base–base stacking does not affect the electron affinities of dCpdG and dGpdC. The density functional B3LYP,[62–64] which does not include the stacking interaction, and the density functional M05-2X,[65–66] which does replicate the stacking interaction, provide almost the same electron affinities for dCpdG and dGpdC.[60] Moreover, computational studies of the double-stranded model of the deoxyadenylyl-3′,5′-deoxyuridine illustrated that the DFT approach is able to achieve the structure consistent with experiment when the major elements of environments are incorporated.[61] Therefore, the B3LYP functional approach[36,37] was adopted in this study in order to maintain consistency with our previous studies of electron attachment to DNA subunits. Basis sets of double-ζ quality, plus polarization and diffuse functions (6-31+G(d,p)), were used to obtain optimized geometries and natural charges for the model molecules in both neutral and anionic forms. Previous studies[31,37,38] have shown that the B3LYP/6-31+G(d,p) approach predicts electron affinities for the DNA components very close to those predicted by the B3LYP functional with a slightly larger basis set, DZP++. To ensure consistency with our previous studies, the DZP++ basis set was also used to evaluate the energy of the complexes based on the structures optimized at the B3LYP/6-31+G(d,p) level of theory. The DZP++ basis sets were constructed by augmenting the Huzinaga–Dunning[67,68] set of contracted double-ζ Gaussian functions, with one set of p-type polarization functions along with one even-tempered diffuse s function for each H atom, and one set of five d-

type polarization functions in addition to sets of even-tempered diffuse s and p functions for each C, N, O, and P atom. The even-tempered orbital exponents were determined according to the prescription of Lee.[69] Each adiabatic electron affinity was computed as the difference between the absolute energies of the appropriate neutral and anion species at their respective optimized geometries: $AEA = E_{neut} - E_{anion}$.

To evaluate the electron-capture abilities of DNA double strands in aqueous solution, a polarizable continuum model (PCM)[70] with the dielectric constant of water ($\varepsilon = 78.39$) was used to simulate the polarizable medium environment of an aqueous solution. To analyze the distribution of each unpaired electron, molecular orbital and spin density plots were constructed from the corresponding B3LYP/6-31+G(d,p) densities. Natural population analyses (NPAs) were determined using the B3LYP functional and the 6-31+G(d,p) basis set with the natural bond orbital (NBO) method of Reed and Weinhold.[71,72] The GAUSSIAN 03 system of DFT programs[73] was used for all computations.

Results and Discussion

Geometries: The fully optimized geometries for the neutral and anionic dGpdC dimer octahydrate are depicted in Figures 1 and 2. The lengths of the hydrogen bonds between the nucleotide pairs are summarized in Table 1. It is important to note that, although the B3LYP approach does not account for dispersion interactions between the nucleobases, the optimized structure of the dGpdC dimer complex in the neutral form exhibits the typical geometrical characteristics of stacked bases. The angle between the plane of C1 and the plane of G2 is 17.9°, and the base-plane angle between G1 and C2 is 6.9°. Clearly, the hydrogen-bonding networks through the hydration water molecules account for this near-parallel base–base stacking mode. On the other hand, the hydration pattern seems to attenuate the hydrogen bonding between the bases. The distances for the hydrogen bonding between C1 and G1 are 1.833 Å for H(N4)···O6 (r_1), 1.983 Å for N3···H(N1) (r_2), and 1.995 Å for O2···H(N2) (r_3) in the dGpdC dimer octahydrate, about 0.1 Å shorter than the corresponding hydrogen bonds in the dC:dG nucleoside pair.[42] Similar hydrogen bond lengths are also found between C2 and G2 in the dGpdC dimer octahydrate (see Table 1). As expected, without dispersion interactions, the distance between the bases are relatively larger (4.66 Å for the distance between the center of C1 and the plane of G2, and 4.42 Å for the distance between the center of C2 and the plane of G1).

Electron attachment to the dGpdC dimer octahydrate (forming the radical anion $[dGpdC]_2^{\bullet-}$) leads to a twisted helical structure. The base-plane of C1 and G1 tilts with an angle of 40.2°, and that of C2 and G2 tilts with an angle of 35.5°. The short hydrogen bond between N3 of C1 and H(N1) of G1 ($r_2 = 1.728$ Å) suggests that the excess electron resides mainly on the base C1. This electron, located on C1, also results in a longer base–base stacking distance. In $[dGpdC]_2^{\bullet-}$, the center of C1 is 5.23 Å away from the plane of G2, about 0.57 Å further than for the neutral species.

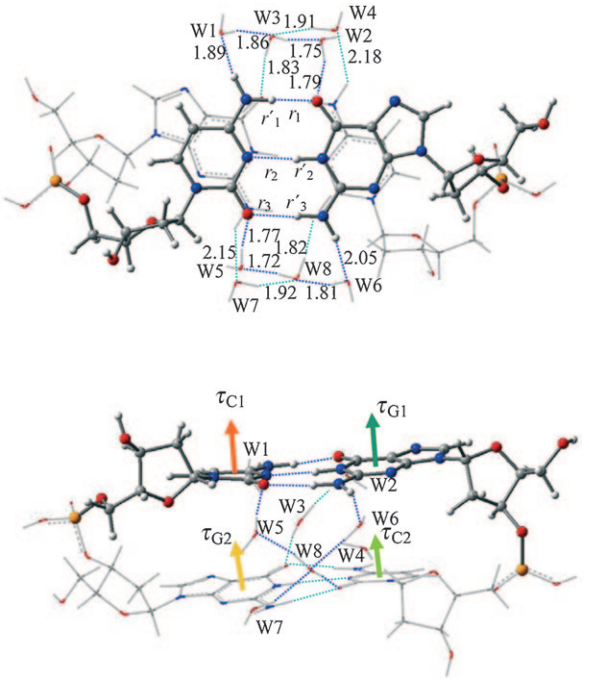

Figure 1. Two views of the optimized geometrical structure for the neutral dGpdC dimer octahydrate. Bond lengths are in Å. Color representations: orange for P, gray for C, red for O, blue for N, and white for H.

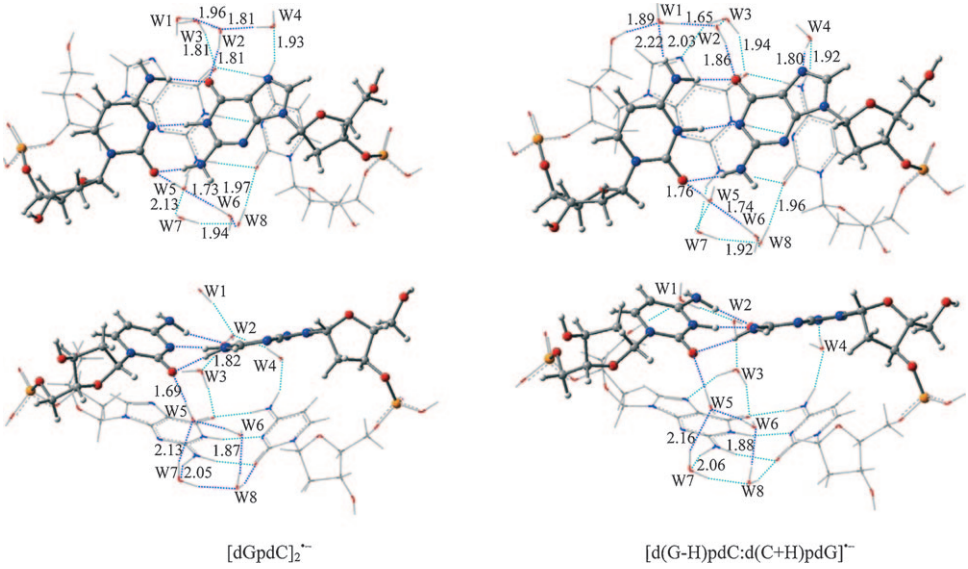

Figure 2. Optimized geometrical structures for the radical anions of the dGpdC dimer octahydrate. Bond lengths are in Å. Color representations: orange for P, gray for C, red for O, blue for N, and white for H.

Table 1. The hydrogen bond lengths between the bases, the base-plane distance between the stacked bases, and the angle of the base-planes between the bases.[a]

Species	$[dGpdC]_2$	$[dGpdC]_2^{\bullet-}$	$[d(G-H)pdC:d(C+H)pdG]^{\bullet-}$
r_1 [Å]	1.833	2.032 (1.967)[b]	1.902 (1.714)[b]
r_2 [Å]	1.983	1.728 (1.777)[b]	1.789 (1.817)[b]
r_3 [Å]	1.995	1.823 (1.657)[b]	2.070 (1.956)[b]
r'_1 [Å]	1.830	1.863	1.849
r'_2 [Å]	1.932	1.936	1.923
r'_3 [Å]	1.909	1.931	1.952
R_{C1G2} [Å]	4.664	5.225	5.417
R_{C2G1} [Å]	4.421	4.551	4.789
θ_{C1G2} [°]	17.9	8.2	14.1
θ_{C2G1} [°]	6.9	33.3	32.4
θ_{C1G1} [°]	10.4	40.2	41.7
θ_{C2G2} [°]	14.1	35.5	40.2

[a] Base-plane distance is defined as the distance between the geometrical center formed by N1N3C5 of cytosine and the base-plane formed by N1N3C5 of guanine. The angle of base-planes is defined as the angle between the vector determined by N1N3C5 of cytosine (τ_C, see Figure 1) and the vector determined by N1N3C5 of guanine (τ_G, see Figure 1). [b] Radical anions of the dG:dC nucleoside pair, see ref. [42].

Meanwhile, the distance between the center of C2 and the plane of G1 is 4.55 Å in the radical anion $[dGpdC]_2^{\bullet-}$, similar to that for $[dGpdC]_2$.

Studies of the radical anions of the G:C pair[37,40] and the dG:dC pair[42] revealed that electron attachment to the guanine-paired cytosine complexes might trigger interbase proton transfer, that is, the proton at the N1 of G migrates to the electron-residing cytosine, forming the radical anion $[d(G-H):d(C+H)]^{\bullet-}$, which is more stable than the canonical form $[dG:dC]^{\bullet-}$.[42] Similarly, the interstrand proton-transferred structure of the radical anion of $[dGpdC]_2$ (denoted as $[d(G-H)pdC:d(C+H)pdG]^{\bullet-}$, see Figure 2) has also been located. Except for the H(N1) of G1 being transferred to the N3 of C1 (causing the bond length variations in the interstrand hydrogen bonding), the overall geometrical parameters of $[d(G-H)pdC:d(C+H)pdG]^{\bullet-}$ are similar to those for $[dGpdC]_2^{\bullet-}$. Due to the proton transfer, the H(N4)···O6 (r_1) bond length decreases to 1.902 Å, and the H(N3)···N1 (r_2) bond length decreases to 1.789 Å, whereas the O2···H(N2) (r_3) bond length increases to 2.070 Å in $[d(G-H)pdC:d(C+H)pdG]^{\bullet-}$. Compared with the interbase hydrogen-bonding features in previous studies of the radical anions of G:C and dG:dC pairs, the interstrand hydrogen bond lengths of $[d(G-H)pdC:d(C+H)pdG]^{\bullet-}$ confirm that the unpaired electron still resides on the (C+H) moiety in the complex. On the other hand, the negative charge is now located on the N1 deprotonated guanine moiety, owing to the interstrand proton transfer.

It is interesting to note that the microhydration pattern in the optimized structure of the neutral form of the dGpdC dimer octahydrate is very similar to that found in the crystal structure of the RNA double-helical fragment of guanylyl-3′,5′-cytidine.[74] Although the hydrogen-bonding network through this microhydration pattern is important for the formation of the stacked form of the dGpdC dimer, our preliminary studies of the dry form of the DNA segments imply that this hydrogen-bonding network is not always necessary if the stacking interactions have been properly introduced.

Electron affinities and energetic properties: The significant positive electron affinities (Table 2) of the present model system suggest that the dGpdC dimer has a strong tendency to capture excess electrons and form an electronically stable radical anion.

At the B3LYP/6-31+G(d,p) level of theory, the adiabatic electron affinity of the microsolvated $[dGpdC]_2$ is predicted to be 1.14 eV (1.19 eV from a single-point calculation with the DZP++ basis set). Compared to the AEA of the microhydrated single-strand dGpdC (0.66 eV), the AEA of the double-strand helical form of $[dGpdC]_2$ increases greatly. The presence of the pairing guanosine increases the AEA by 0.48 eV. A similar increase has also been found in the AEAs of the G:C and dG:dC pairs. The pairing effects on the AEA are affected slightly by the sizes of the models (the AEA increases by 0.53 eV for G:C, 0.47 eV for dG:dC, and 0.48 eV for $[dGpdC]_2$, respectively, as compared to the corresponding unpaired species).

Table 2. Electron affinities of cytosine-containing nucleic acid base, nucleoside, nucleotides, oligonucleotides, and the corresponding pairs [eV].[a]

Process	AEA	VEA[b]	VDE[c]
$[dGpdC]_2 \rightarrow [dGpdC]_2^{\bullet-}$	1.14 (**1.19**, *1.13*)	0.38	2.20 (**2.21**)
$[dGpdC]_2 \rightarrow [d(G-H)pdC:d(C+H)pdG]^{\bullet-}$	1.66 (**1.71**)		2.74 (**2.76**)
$dGpdC \rightarrow [dGpdC]^{\bullet-}$	0.66[d]	0.25[d]	1.42[d]
$dCpdG \rightarrow [dCpdG]^{\bullet-}$	0.90[d]	0.16[d]	1.64[d]
3′,5′-dCDP→[3′,5′-dCDP]$^{\bullet-}$	0.27[e]	0.03[e]	0.71[e]
3′-dCMP→[3′-dCMP]$^{\bullet-}$	0.33[f]	0.15[f]	1.28[f]
$dG:dC \rightarrow dG:dC^{\bullet-}$	0.68[g]	0.16[g]	
$G:C \rightarrow G:C^{\bullet-}$	0.44[h]	0.03[h]	
$dC \rightarrow dC^{\bullet-}$	0.21[i]	−0.09[i]	0.72[i]
$C \rightarrow C^{\bullet-}$	−0.09[j]		

[a] Plain print is used for results obtained with the B3LYP/6-31+G(d,p); **bold**: single point with B3LYP/DZP++; *italics*: optimized with M05-2X/6-31+G(d,p). [b] VEA = E(neutral) − E(anion); the energies are evaluated using the optimized neutral structures. [c] VDE = E(neutral) − E(anion); the energies are evaluated using the optimized anion structures. [d] Ref. [60]. [e] Ref. [18]. [f] Refs. [17,34], in which 3′-dCMP was labeled as 3′-dCMPH. [g] Ref. [42]. [h] Ref. [31]. [i] Ref. [16]. [j] Refs. [16,30].

The estimation of the vertical electron attachment energies (VEAs) is important in order to explore the electron-capturing behavior of DNA at the nascent stage of electron attachment. The substantial VEA predicted for the microsolvated dGpdC dimer (0.38 eV) in the present investigation indicates that the cytosine- and guanine-rich nucleotide duplexes are reasonable electron captors. In comparison, a smaller VEA value has been predicted by the B3LYP approach for the microsolvated oligonucleotide dGpdC

(0.25 eV). The increase in the VEA of $[dGpdC]_2$ suggests that the pairing of the guanosine is a critical factor for improving the effective electron-capturing abilities of DNA double strands.

The vertical detachment energies (VDE) help assess the electronic stability of radical anions, and are most readily determined by anion photodetachment experiments.[19,26,28] The VDE of the radical anion $[dGpdC]_2^{\bullet-}$ has been predicted here in order to evaluate its electronic stability. The VDE is found to be 2.20 eV for $[dGpdC]_2^{\bullet-}$, significantly larger than those for the single-strand oligonucleotides (1.42 eV for $[dGpdC]^{\bullet-}$ and 1.64 eV for $[dCpdG]^{\bullet-}$). Because this VDE value is far larger than the activation energy barrier needed for the interstrand proton transfer (2.4 kcal mol^{-1}, or 0.1 eV for the radical anion of dG:dC),[42] the proton transfer from N1 of G1 to N3 of C1 should take place without causing the detachment of the excess electron from the radical anion $[dGpdC]_2^{\bullet-}$.

Interstrand proton transfer between N1 of G1 and N3 of C1 of the radical anion $[dGpdC]_2^{\bullet-}$ results in an even more stable radical anion $[d(G-H)pdC:d(C+H)pdG]^{\bullet-}$, which lies 12.0 kcal mol^{-1} (0.52 eV) lower than $[dGpdC]_2^{\bullet-}$ in total energy. Notice that the total energy of the proton-transferred radical anion of the nucleoside pair $[d(G-H):d(C+H)]^{\bullet-}$ is only 2.3 kcal mol^{-1} lower than that for $dG:dC^{\bullet-}$, and that the energy difference between $(G-H):d(C+H)^{\bullet-}$ and $G:C^{\bullet-}$ is only 2.9 kcal mol^{-1}. The larger energy difference between the radical anions $[dGpdC]_2^{\bullet-}$ and $[d(G-H)pdC:d(C+H)pdG]^{\bullet-}$ should partly be attributed to the influence of microhydration. Interstrand proton transfer also increases the electronic stability of the radical anion of $[dGpdC]_2$. The vertical detachment energy of $[d(G-H)pdC:d(C+H)pdG]^{\bullet-}$ is predicted to be 2.74 eV, which is 0.54 eV higher than that of $[dGpdC]_2^{\bullet-}$. Considering that the neutral radical $d(C+H)^{\bullet}$ has been suggested to be a good electron acceptor, $[d(G-H)pdC:d(C+H)pdG]^{\bullet-}$ might receive a second electron to form a dianion in its microhydrated form, and, therefore, trigger the formation of abasic sites in DNA duplexes. It is important to note that Chen et al. reached the same conclusion in their study of the GC pair embedded in B-form DNA.[75]

Analogous to the nucleotides and the DNA single strands, interaction with water greatly improves the electron-capture ability of DNA double strands.[8,17–19,35] Note that the term "electron affinity" for a solvated molecule M implies that the physical situation described is a microsolvated $M(H_2O)_n$ system, in which the waters enclose M uniformly, and n becomes arbitrarily large. Meanwhile, there is no proton exchanging between M and solvent. In this sense, the AEA is 2.03 eV for DNA duplex segment $[dGpdC]_2$ in aqueous solution (see Table 3). Noting that the extra electron is mainly localized on one of the cytosine nucleobases (see below), the AEA value of 2.03 eV should be the ultimate electron affinity value of cytosine in DNA duplexes. Compared to the microsolvated $[dGpdC]_2$ octahydrate, the increase of the AEA in aqueous solution amounts to about 0.9 eV. Similarly, the increase of the AEA in aqueous solution is 1.01 eV for the microhydrated single-strand oligonucleotides dGpdC and dCpdG. Interaction with the polarizable medium enhances the electron-capture ability of the helical form of $[dGpdC]_2$. The vertical attachment energy of $[dGpdC]_2$ has been estimated to be 1.48 eV in the presence of the polarizable continuum. The polarizable medium also greatly enhances the electronic stability of the radical anions. The VDEs of $[dGpdC]_2^{\bullet-}$ and $[d(G-H)pdC:d(C+H)pdG]^{\bullet-}$ increase to 2.70 and 3.26 eV, respectively, in the PCM model. In the PCM simulations the proton-transferred radical anion $[d(G-H)pdC:d(C+H)pdG]^{\bullet-}$ is still more stable than $[dGpdC]_2^{\bullet-}$ from the perspective of the total energy. Therefore, experimental detection of evidence for electron attachment to DNA double helices in aqueous solution should be related to the $[d(G-H)pdC:d(C+H)pdG]^{\bullet-}$ complexes.

Table 3. "Electron affinities" of nucleotides in aqueous solution.[a]

Process	AEA [eV]	VDE [eV]
$[dGpdC]_2 \rightarrow [dGpdC]_2^{\bullet-}$	2.03	2.70
$[dGpdC]_2 \rightarrow [d(G\text{-}H)pdC:d(C+H)pdG]^{\bullet-}$	2.26	3.26
$dGpdC \rightarrow [dGpdC]^{\bullet-}$	1.65	2.58
$dCpdG \rightarrow [dCpdG]^{\bullet-}$	1.91	2.74
$3',5'\text{-dCDP} \rightarrow [3',5'\text{-dCDP}]^{\bullet-}$	1.99[b]	
$5'\text{-dCMP} \rightarrow [5'\text{-dCMP}]^{\bullet-}$	1.89[c]	
$3'\text{-dCMP} \rightarrow [3'\text{-dCMP}]^{\bullet-}$	2.18[d]	

[a] Results obtained with the B3LYP/6-31+G(d,p) approach. [b] Ref. [18]. [c] Ref. [8]. [d] Refs. [17,34].

Charge distributions and molecular orbital analysis: The distribution of negative charge on the constituent parts of the oligonucleotide duplex also provides some insight into the overall electronic effect of the charge. Table 4 summarizes the charge distributions among the bases, ribose, phosphates, and hydration waters for both the neutral and anionic complexes. Analysis of the NPA charge differences between the neutral and anionic nucleotides supports the conclusion that the excess electron mainly resides one of nucleobase cytosine moieties in the radical anion $[dGpdC]_2^{\bullet-}$ before the interstrand proton transfer, whereas it is mainly located at the deprotonated guanine moiety in $[d(G-H)pdC:d(C+H)pdG]^{\bullet-}$ following the proton transfer. The NPA charge differences suggest that there is 0.73 a.u. of "extra negative charge" located on the cytosine (C1), and 0.11 a.u. on the C1-connected ribose of $[dGpdC]_2^{\bullet-}$. About 0.05 e^- of extra negative charge is found to reside on the base guanine (G1), which is paired with C1 through three pairs of hydrogen bonds, in $[dGpdC]_2^{\bullet-}$. Conversely, the charge distribution differences of the interstrand proton-transferred radical anion $[d(G-H)pdC:d(C+H)pdG]^{\bullet-}$ show significant increases in the negative charge resident on the deprotonated G1 (0.77 a.u. of the extra negative charge), and only 0.04 a.u. of the extra negative charge populations on the base moieties of cytosine. The singly-occupied molecular orbitals (SOMOs) demonstrate that the unpaired electron is located mainly on C1 in both $[dGpdC]_2^{\bullet-}$ and $[d(G-H)pdC:d(C+H)pdG]^{\bullet-}$ (Figure 3). Considering that the excess negative charge resides mainly on G1 of $[d(G-H)pdC:d$-

Table 4. NPA charge distributions of the neutral and radical anion forms of $[dGpdC]_2$.[a]

Component	Neutral	Anion (V)[b]	Anion1	Anion2
GAS				
C1	−0.244	−0.483 (−0.239)	−0.977 (−0.733)	−0.287 (−0.043)
C2	−0.224	−0.487 (−0.263)	−0.260 (−0.036)	−0.269 (−0.045)
G1	−0.304	−0.322 (−0.018)	−0.352 (−0.048)	−1.075 (−0.771)
G2	−0.299	−0.316 (−0.017)	−0.311 (−0.012)	−0.306 (−0.007)
ribose (C1)	0.644	0.603 (−0.031)	0.531 (−0.113)	0.560 (−0.084)
ribose (C2)	0.605	0.548 (−0.057)	0.629 (0.024)	0.635 (0.030)
ribose (G1)	0.611	0.589 (−0.022)	0.593 (−0.018)	0.599 (−0.012)
ribose (G2)	0.614	0.576 (−0.038)	0.636 (0.022)	0.621 (0.007)
phosphate (L)[c]	−0.687	−0.846 (−0.159)	−0.710 (−0.023)	−0.712 (−0.025)
phosphate (R)[c]	−0.687	−0.820 (−0.133)	−0.690 (−0.003)	−0.694 (−0.007)
water (U)[d]	−0.009	−0.016 (−0.007)	−0.044 (−0.035)	−0.041 (−0.032)
water (D)[d]	−0.020	−0.027 (−0.007)	−0.043 (−0.023)	−0.032 (−0.012)
PCM				
C1	−0.246	−0.548 (−0.302)	−0.994 (−0.748)	−0.307 (−0.061)
C2	−0.232	−0.690 (−0.458)	−0.268 (−0.036)	−0.278 (−0.046)
G1	−0.327	−0.392 (−0.065)	−0.370 (−0.043)	−1.097 (−0.770)
G2	−0.324	−0.401 (−0.077)	−0.327 (−0.003)	−0.319 (0.005)
ribose (C1)	0.665	0.640 (−0.025)	0.563 (−0.102)	0.597 (−0.068)
ribose (C2)	0.631	0.584 (−0.047)	0.656 (0.025)	0.661 (0.030)
ribose (G1)	0.625	0.620 (−0.005)	0.608 (−0.017)	0.614 (−0.011)
ribose (G2)	0.629	0.623 (−0.006)	0.642 (0.013)	0.622 (−0.007)
phosphate (L)[c]	−0.694	−0.696 (−0.002)	−0.718 (−0.024)	−0.718(−0.024)
phosphate (R)[c]	−0.695	−0.698 (−0.003)	−0.694 (0.001)	−0.696 (−0.001)
water (U)[d]	−0.014	−0.020 (−0.006)	−0.053 (−0.039)	−0.046 (−0.032)
water (D)[d]	−0.018	−0.023 (−0.005)	−0.046 (−0.028)	−0.033 (−0.015)

[a] NPA charge differences between neutral and anionic species are in parentheses. [b] Anion (V) stands for the vertical-electron-attached radical anion; Anion1 for $[dGpdC]_2^{\bullet-}$, and Anion2 for $[d(G-H)pdC:d(C+H)pdG]^{\bullet-}$. [c] Phosphate(L) linked to Ribose(C1) and Ribose(G2); Phosphate(R) linked to Ribose(G1) and Ribose(C2). [d] Water(U) stands for the four water molecules (W1, W2, W3, and W4) in the major groove, and Water(D) stands for the four water molecules (W5, W6, W7, and W8) in the minor groove.

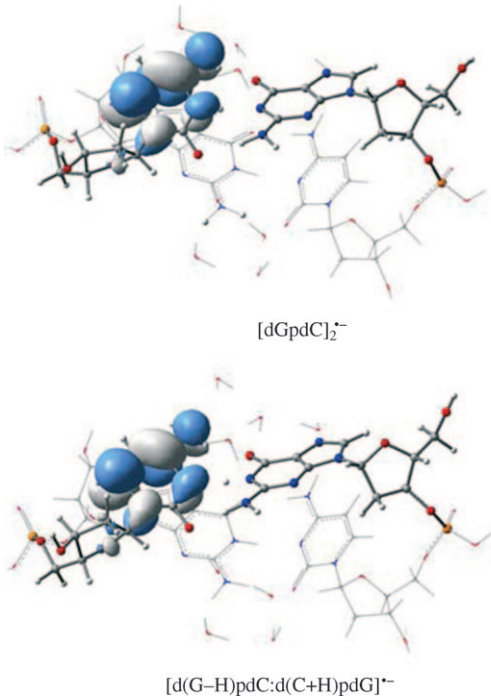

Figure 3. The singly occupied molecular orbitals (SOMOs) of $[dGpdC]_2^{\bullet-}$ and $[d(G-H)pdC:d(C+H)pdG]^{\bullet-}$.

$(C+H)pdG]^{\bullet-}$, this radical anion exhibits the typical characteristics of a distonic radical anion, in which the unpaired electron is well separated from the center of negative charge in the system. This feature further stabilizes the electron-attached $[dGpdC]_2$, and, thus, the intrastrand proton-transferred radical anion $[d(G-H)pdC:d(C+H)pdG]^{\bullet-}$ provides a good illustration of distonic radical anions in biochemistry.

Negative charge has also been found to appear, in a simple picture, on the microhydration waters in these radical anions. The general trend is that the hydration waters in the major groove accept more negative charge than those in the minor groove.

It is important to note that the extra negative charge distribution spreads to both cytosine bases C1 and C2 in the vertical-electron-attached duplex (the extra negative charge amounts to 0.24 e^- on C1 and 0.26 e^- on C2), whereas it is mainly located on one of the bases of the duplex after geometrical relaxation (i.e., in the optimized structures of the radical anions). This observation is consistent with the character of the SOMO in Figure 4, in which the unpaired electron is predicted to be found on both cytosine bases. Moreover, the extra negative charge also extends to the phosphate groups in the vertical-electron-attached duplex. The NPA analysis shows that about 0.13–0.16 a.u. of

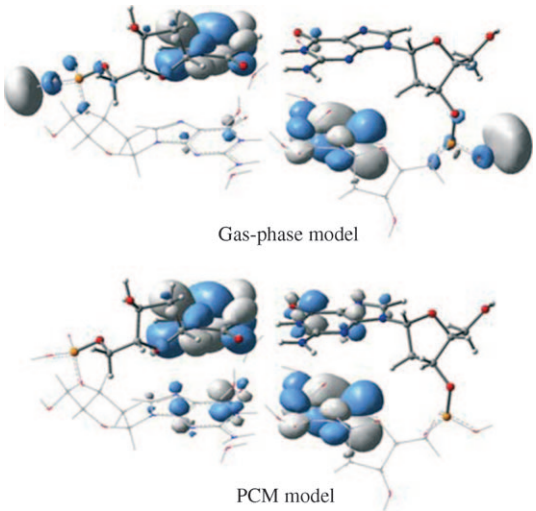

Figure 4. The SOMO of vertical-electron-attached $[dGpdC]_2$ in the gas-phase model and in the PCM model.

the extra negative charge is located around the phosphate moieties. The SOMO of the vertical-electron-attached duplex suggests that these two parts are loosely bound to the extra negative charge.

Including the polarizable continuum in the NPA analysis reveals that the interaction between the polarizable medium and the radical anions has little effect on the charge distribution in the optimized radical anions. However, the solvent effects significantly increase the negative charge accumulation on the two cytosine bases (0.32 and 0.46 e^- of extra negative charge on C1 and C2, respectively, in the PCM model) for the vertical-electron-attached duplex $[dGpdC]_2$ octahydrate. Negative charge accumulation on G1 (0.07 e^-) and G2 (0.08 e^-) of the vertical-electron-attached $[dGpdC]_2$ in aqueous solution is also revealed by the NPA analysis. Meanwhile, the loosely held charge around the phosphate groups in the gas phase is eliminated due to the influence of the polarizable medium. These changes are demonstrated clearly in the SOMO of the corresponding vertical-electron-attached $[dGpdC]_2$ in aqueous solution.

Conclusion

The dinucleoside phosphate deoxyguanylyl-3′,5′-deoxycytidine dimer, $[dGpdC]_2$, is one of the simplest fragments of the DNA duplex that may be considered representative. Exploring electron attachment to this foundational section of DNA helices enables one to approach reliable predictions of the electron-attracting capabilities of DNA double strands.

For the first time the minimal skeletal section of DNA helices, $[dGpdC]_2$, has been constructed, fully optimized, and analyzed by a quantum mechanical approach at a reliable level of theory (the B3LYP version that reproduces the experimental EA values for both nucleobases[30,32] and nucleosides[16,28] at a reasonable level of accuracy). The study of the electron-attached $[dGpdC]_2$ reveals that DNA double strands are capable of capturing low-energy electrons and forming electronically stable radical anions. The relatively large vertical electron affinity (VEA) predicted for $[dGpdC]_2$ (0.38 eV) and the charge distribution analysis, along with the molecular orbitals for the vertical-electron-attached $[dGpdC]_2$ complex, indicate that the cytosine bases are good electron captors in DNA double strands.

The structure, charge distribution, and molecular orbital analysis for the fully optimized radical anion $[dGpdC]_2^{\bullet-}$ suggest that, accompanying geometrical relaxation, the extra electron tends to redistribute to one of the cytosine base moieties, in an electronically stable structure (with adiabatic electron affinity (AEA) 1.14 eV and vertical detachment energy (VDE) 2.20 eV).

The effects of the polarizable medium have been found to be important for increasing the electron-capture ability of the dGpdC dimer. With the PCM model, the ultimate AEA value of cytosine in DNA duplexes is predicted to be about 2.0 eV in aqueous solution.

The structural features of the optimized radical anion $[dGpdC]_2^{\bullet-}$ also strongly suggest the possibility of interstrand proton transfer. The interstrand proton transfer leads to a distonic radical anion $[d(G-H)pdC:d(C+H)pdG]^{\bullet-}$, which contains one deprotonated guanine anion and one protonated cytosine radical. This distonic radical anion is predicted to be more stable than $[dGpdC]_2^{\bullet-}$ in situations either with or without the interaction due to the polarizable continuum. Therefore, experimental evidence for electron attachment to DNA double helices should be related to $[d(G-H)pdC:d(C+H)pdG]^{\bullet-}$ complexes, for which the VDE might be high as 2.7 eV (dry conditions) to 3.3 eV (fully hydrated conditions).

Acknowledgements

This research was supported by the U.S. National Science Foundation, Grant CHE-0749868. In China it was supported by the National Science & Technology Major Project "Key New Drug Creation and Manufacturing Program", China (Number: 2009ZX09301-001).

[1] D. Becker, M. D. Sevilla, *Advances in Radiation Biology, Vol. 17* (Ed.: J. Lett), Academic Press, New York, **1993**, pp. 121–180.
[2] S. O. Kelley, J. K. Barton, *Science* **1999**, *283*, 375–381.
[3] M. Ratner, *Nature* **1999**, *397*, 480–481.
[4] B. Boudaiffa, P. Cloutier, D. Hunting, M. A. Huels, L. Sanche, *Science* **2000**, *287*, 1658–1659.
[5] X. Pan, P. Cloutier, D. Hunting, L. Sanche, *Phys. Rev. Lett.* **2003**, *90*, 208102.
[6] G. L. Caron, L. Sanche, *Phys. Rev. Lett.* **2003**, *91*, 113201.
[7] Y. Zheng, P. Cloutier, D. Hunting, J. R. Wagner, L. Sanche, *J. Am. Chem. Soc.* **2004**, *126*, 1002–1003.
[8] X. Bao, J. Wang, J. Gu, J. Leszczynski, *Proc. Natl. Acad. Sci. USA* **2006**, *103*, 5658–5663.
[9] D. B. Hall, R. E. Holmlin, J. K. Barton, *Nature* **1996**, *382*, 731–735.
[10] S. Steenken, *Biol. Chem.* **1997**, *378*, 1293–1297.
[11] G. Taubes, *Science* **1997**, *275*, 1420–1421.
[12] Y. A. Berlin, A. L. Burin, M. A. Ratner, *J. Am. Chem. Soc.* **2001**, *123*, 260–268.
[13] D. Beljonne, G. Pourtois, M. A. Ratner, J. L. Bredas, *J. Am. Chem. Soc.* **2003**, *125*, 14510–14517.
[14] M. A. Huels, I. Hahndorf, E. Illenberger, L. Sanche, *J. Chem. Phys.* **1998**, *108*, 1309–1312.
[15] S. G. Ray, S. S. Daube, R. J. Naaman, *Proc. Natl. Acad. Sci. USA* **2005**, *102*, 15–19.
[16] N. A. Richardson, J. Gu, S. Wang, Y. Xie, H. F. Schaefer, *J. Am. Chem. Soc.* **2004**, *126*, 4404–4411.
[17] J. Gu, J. Wang, J. Leszczynski, *J. Am. Chem. Soc.* **2006**, *128*, 9322–9323.
[18] J. Gu, Y. Xie, H. F. Schaefer, *Nucleic Acid Res.* **2007**, *35*, 5165–5172.
[19] J. Schiedt, R. Weinkauf, D. M. Neumark, E. W. Schlag, *Chem. Phys.* **1998**, *239*, 511–524.
[20] B. F. Parsons, S. Sheehan, T. A. Yen, *Phys. Chem. Chem. Phys.* **2007**, *9*, 3291–3297.
[21] D. Desfrancois, Abdoul-H. Carime, J. P. Schermann, *J. Chem. Phys.* **1996**, *104*, 7792–7794.
[22] V. Periquet, A. Moreau, S. Carles, J. P. Schermann, *J. Electron Spectrosc. Relat. Phenom.* **2000**, *106*, 141–151.
[23] M. Gutowski, I. Dabkowska, J. Rak, S. Xu, J. M. Nilles, D. Radisic, K. H. Bowen, *Eur. Phys. J. D* **2002**, *20*, 431–439.
[24] M. Haranczyk, M. Gutowski, X. Li, K. H. Bowen, *Proc. Natl. Acad. Sci. USA* **2007**, *104*, 4804–4807.

[25] M. Haranczyk, M. Gutowski, X. Li, K. H. Bowen, *J. Phys. Chem. B* **2007**, *111*, 14073–14076.
[26] D. Radisic, K. H. Bowen, I. Dabkowska, P. Storoniak, J. Rak, M. Gutowski, *J. Am. Chem. Soc.* **2005**, *127*, 6443–6450.
[27] N. A. Richardson, S. S. Wesolowski, H. F. Schaefer, *J. Phys. Chem. B* **2003**, *107*, 848–853.
[28] S. T. Stokes, X. Li, A. Grubisic, Y. J. Ko, K. H. Bowen, *J. Chem. Phys.* **2007**, *127*, 084321.
[29] M. Haranczyk, M. Gutowski, *Angew. Chem.* **2005**, *117*, 6743–6746; *Angew. Chem. Int. Ed.* **2005**, *44*, 6585–6588.
[30] S. S. Wesolowski, M. L. Leininger, P. N. Pentchev, H. F. Schaefer, *J. Am. Chem. Soc.* **2001**, *123*, 4023–4028.
[31] X. Li, M. D. Sevilla, L. Sanche, *J. Am. Chem. Soc.* **2003**, *125*, 8916–8920.
[32] F. Ban, M. J. Lundqvist, R. J. Boyd, L. A. Eriksson, *J. Am. Chem. Soc.* **2002**, *124*, 2753–2761.
[33] J. C. Rienstra-Kiracofe, G. S. Tschumper, H. F. Schaefer, S. Nandi, G. B. Ellison, *Chem. Rev.* **2002**, *102*, 231–282.
[34] J. Gu, Y. Xie, H. F. Schaefer, *J. Am. Chem. Soc.* **2006**, *128*, 1250–1252.
[35] J. Gu, Y. Xie, H. F. Schaefer, *ChemPhysChem* **2006**, *7*, 1885–1887.
[36] J. Gu, Y. Xie, H. F. Schaefer, *J. Am. Chem. Soc.* **2005**, *127*, 1053–1057.
[37] X. Li, Z. Cai, M. D. Sevilla, *J. Phys. Chem. B* **2001**, *105*, 10115–10123.
[38] X. Li, Z. Cai, M. D. Sevilla, *J. Phys. Chem. A* **2002**, *106*, 9345–9351.
[39] J. Reynisson, S. Steenken, *Phys. Chem. Chem. Phys.* **2002**, *4*, 5353–5358.
[40] N. A. Richardson, S. S. Wesolowski, H. F. Schaefer, *J. Am. Chem. Soc.* **2002**, *124*, 10163–10170.
[41] J. Gu, Y. Xie, H. F. Schaefer, *J. Phys. Chem. B* **2005**, *109*, 13067–13075.
[42] J. Gu, Y. Xie, H. F. Schaefer, *J. Chem. Phys.* **2007**, *127*, 155107.
[43] J. Gu, Y. Xie, H. F. Schaefer, *J. Phys. Chem. B* **2006**, *110*, 19696–19703.
[44] J. Smets, W. McCarthy, L. Adamowicz, *J. Phys. Chem.* **1996**, *100*, 14655–14660.
[45] J. Smets, D. M. A. Smith, Y. Elkadi, L. Adamowicz, *J. Phys. Chem. A* **1997**, *101*, 9152–9156.
[46] O. Dolgounitcheva, V. G. Zakrzewski, J. V. Ortiz, *J. Phys. Chem. A* **1999**, *103*, 7912–7917.
[47] A. Morgado, K. Pichugin, L. Adamowicz, *Phys. Chem. Chem. Phys.* **2004**, *6*, 2758–2762.
[48] A. Kumar, P. C. Mishra, S. Suhai, *J. Phys. Chem. A* **2005**, *109*, 3971–3979.
[49] X. Bao, H. Sun, N. Wong, J. Gu, *J. Phys. Chem. B* **2006**, *110*, 5868–5874.
[50] X. Bao, G. Liang, N. Wong, J. Gu, *J. Phys. Chem. A* **2007**, *111*, 666–672.
[51] A. O. Colson, B. Besler, M. D. Sevilla, *J. Phys. Chem.* **1993**, *97*, 13852–13859.
[52] M. D. Sevilla, B. B. Besler, A. O. Colson, *J. Phys. Chem.* **1994**, *98*, 2215.
[53] J. H. Hendricks, S. A. Lyapustina, H. L. de Clercq, K. H. Bowen, *J. Chem. Phys.* **1998**, *108*, 8–11.
[54] M. L. Nugent, L. Adamowicz, *Mol. Phys.* **2005**, *103*, 1467–1472.
[55] S. Kim, H. F. Schaefer, *J. Chem. Phys.* **2006**, *125*, 144305.
[56] S. Kim, S. E. Wheeler, H. F. Schaefer, *J. Chem. Phys.* **2006**, *124*, 204310.
[57] S. Kim, H. F. Schaefer, *J. Chem. Phys.* **2007**, *126–127*, 064301.
[58] M. Kobylecka, J. Jeszczynski, J. Rak, *J. Am. Chem. Soc.* **2008**, *130*, 15683–15687.
[59] M. Kobylecka, J. Jeszczynski, J. Rak, *J. Chem. Phys.* **2009**, *131*, 085103.
[60] J. Gu, Y. Xie, H. F. Schaefer, *Chem. Phys. Lett.* **2009**, *473*, 213–219.
[61] C. Fonseca Guerra, F. M. Bickelhaupt, J. G. Snijders, E. J. Baerends, *J. Am. Chem. Soc.* **2000**, *122*, 4117–4128.
[62] A. D. Becke, *J. Chem. Phys.* **1993**, *98*, 5648–5652.
[63] C. Lee, W. Yang, R. G. Parr, *Phys. Rev. B* **1988**, *37*, 785–789.
[64] A. D. Becke, *J. Chem. Phys.* **1993**, *98*, 1372–1377.
[65] Y. Zhao, D. G. Truhlar, *Acc. Chem. Res.* **2008**, *41*, 157–167.
[66] Y. Zhao, N. E. Schultz, D. G. Truhlar, *J. Chem. Theory Comput.* **2006**, *2*, 364–382.
[67] S. Huzinaga, *J. Chem. Phys.* **1965**, *42*, 1293–1302.
[68] T. H. Dunning, *J. Chem. Phys.* **1970**, *53*, 2823–2833.
[69] T. J. Lee, H. F. Schaefer, *J. Chem. Phys.* **1985**, *83*, 1784–1794.
[70] M. Cossi, V. Barone, R. Cammi, J. Tomasi, *Chem. Phys. Lett.* **1996**, *255*, 327–335.
[71] A. E. Reed, P. R. Schleyer, *J. Am. Chem. Soc.* **1990**, *112*: 1434–1445.
[72] A. E. Reed, L. A. Curtiss, *Chem. Rev.* **1988**, *88*, 899–926.
[73] Gaussian 03, Revision E.01, M. J. Frisch, G. W. Trucks, H. B. Schlegel, G. E. Scuseria, M. A. Robb, J. R. Cheeseman, J. A. Montgomery, Jr., T. Vreven, K. N. Kudin, J. C. Burant, J. M. Millam, S. S. Iyengar, J. Tomasi, V. Barone, B. Mennucci, M. Cossi, G. Scalmani, N. Rega, G. A. Petersson, H. Nakatsuji, M. Hada, M. Ehara, K. Toyota, R. Fukuda, J. Hasegawa, M. Ishida, T. Nakajima, Y. Honda, O. Kitao, H. Nakai, M. Klene, X. Li, J. E. Knox, H. P. Hratchian, J. B. Cross, V. Bakken, C. Adamo, J. Jaramillo, R. Gomperts, R. E. Stratmann, O. Yazyev, A. J. Austin, R. Cammi, C. Pomelli, J. W. Ochterski, P. Y. Ayala, K. Morokuma, G. A. Voth, P. Salvador, J. J. Dannenberg, V. G. Zakrzewski, S. Dapprich, A. D. Daniels, M. C. Strain, O. Farkas, D. K. Malick, A. D. Rabuck, K. Raghavachari, J. B. Foresman, J. V. Ortiz, Q. Cui, A. G. Baboul, S. Clifford, J. Cioslowski, B. B. Stefanov, G. Liu, A. Liashenko, P. Piskorz, I. Komaromi, R. L. Martin, D. J. Fox, T. Keith, M. A. Al-Laham, C. Y. Peng, A. Nanayakkara, M. Challacombe, P. M. W. Gill, B. Johnson, W. Chen, M. W. Wong, C. Gonzalez, J. A. Pople, Gaussian, Inc., Wallingford CT, 2004.
[74] W. Saenger, *Principles of Nucleic Acid Structure*, Springer, New York, **1983**.
[75] H. C. Chen, S. C. N. Kao Hsu, *J. Am. Chem. Soc.* **2009**, *131*, 15930–15938.

Received: May 14, 2010
Published online: October 4, 2010

